Macromolecules

Article

Cite This: Macromolecules 2019, 52, 2778−2788

pubs.acs.org/Macromolecules

Multivalency in a Dendritic Host−Guest System

A. F. Smeijers,[†] Koen Pieterse,[†,‡] Peter A. J. Hilbers,[†,‡] and Albert J. Markvoort*[,†,‡]

[†]Computational Biology Group, Department of Biomedical Engineering, and [‡]Institute for Complex Molecular Systems, Eindhoven University of Technology, P.O. Box 513, 5600 MB Eindhoven, The Netherlands

Supporting Information

ABSTRACT: Multivalency is an important instrument in the supramolecular chemistry toolkit for the creation of strong specific interactions. In this paper we investigate the multivalency effect in a dendritic host−guest system using molecular dynamics simulations. Specifically, we consider urea−adamantyl decorated poly(propyleneimine) dendrimers that together with compatible mono-, bi-, and tetravalent ureidoacetic acid guests can form dynamic patchy nanoparticles. First, we simulate the self-assembly of these particles into macromolecular nanostructures, showing guest-controlled reduction of dendrimer aggregation. Subsequently, we systematically study guest concentration dependent multivalent binding. At low guest concentrations multivalency of the guests clearly increases relative binding as tethered headgroups bind more often than free guests' headgroups. We find that despite an abundance of binding sites, most of the tethered headgroups bind in close proximity, irrespective of the spacer length; nevertheless, longer spacers do increase binding. At high guest concentrations the dendrimer becomes saturated with bound headgroups, independent of guest valency. However, in direct competition the tetravalent guests prevail over the monovalent ones. This demonstrates the benefit of multivalency at high as well as low concentrations.

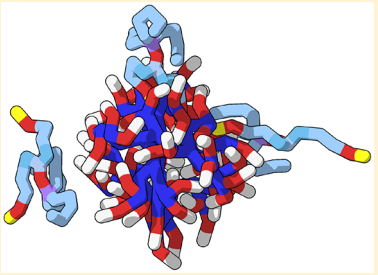

1. INTRODUCTION

For many processes nature relies on reversible noncovalent interactions. To ensure these interactions are sufficiently strong, it often employs the concept of multivalency, i.e., the principle for binding between entities whereby multiple identical ligands bind to multiple identical receptors.[1] Examples of the use of multivalency include the adhesion of viruses to host cells and the binding of antibodies to pathogens. Not only is it in evolutionary terms often easier to multiply a weak interaction to yield a strong collective one than to newly construct a stronger one, it also allows for enhanced specificity in the binding. The concept of multivalency is nowadays also applied successfully in supramolecular chemistry to self-assemble novel complexes.[2−4]

One type of molecule often studied in supramolecular chemistry is the dendrimer.[5] Dendrimers are polymers consisting of short branches that grow from a multifunctional core. They are synthesized in a stepwise fashion where in each generation the number of branches is doubled (Figure 1a). This level of control leads to well-defined molecules compared to other polymers. Moreover, their ends can be coupled to various functional groups to create molecules with a definite number of interaction sites with specific properties. The versatility of the dendrimer components and attachments allows for a multitude of applications. For instance, dendrimers have been used as concentrated displays of contrast agent,[5−9] as targeted drug delivery vehicles,[5−8,10,11] as DNA carriers for gene therapy,[6−8,12] as enzyme mimics,[5−7] as biosensors,[6,7] and as building blocks in supramolecular structures.[5,6,13] Many of these applications are examples of host−guest chemistry, employing the dendrimer as a temporary host vehicle for noncovalently bound guest compounds.[5−8]

An interesting example of supramolecular chemistry with dendrimers is provided by urea−adamantyl decorated dendrimers, which aggregate in water due to the hydrophobic nature of their bulky adamantyl end-groups but can be solubilized by coating them with guests featuring ethylene oxide tails.[14,15] When the dendrimer is only partially covered with guests, it forms a complex with both hydrophilic and hydrophobic domains, which facilitates aggregation into larger nanostructures.[16] In contrast to regular anisotropic nanoparticles with static interaction domains—where the formed supramolecular nanostructure is predetermined by the number and shape of these domains[17]—with these dynamic patchy nanoparticles the noncovalent coating offers opportunities to tune the aggregation. That different guest concentrations change the coverage, and thereby the size and branching of the nanostructures, has been observed in cryo-TEM images.[15,16] Exerting control over the nanostructures formed, however, requires thorough understanding of how the nanoparticles are coated with the noncovalently bound guests. The coverage will depend not only on the guest concentration but also on the host−guest interaction. As dendrimers provide a relatively controlled presentation of binding sites on a spherical macromolecule, a way to enhance the dendrimer−guest interaction may be by employing multivalent guests.

Received: November 3, 2018
Revised: March 6, 2019
Published: March 21, 2019

DOI: 10.1021/acs.macromol.8b02357
Macromolecules 2019, 52, 2778−2788

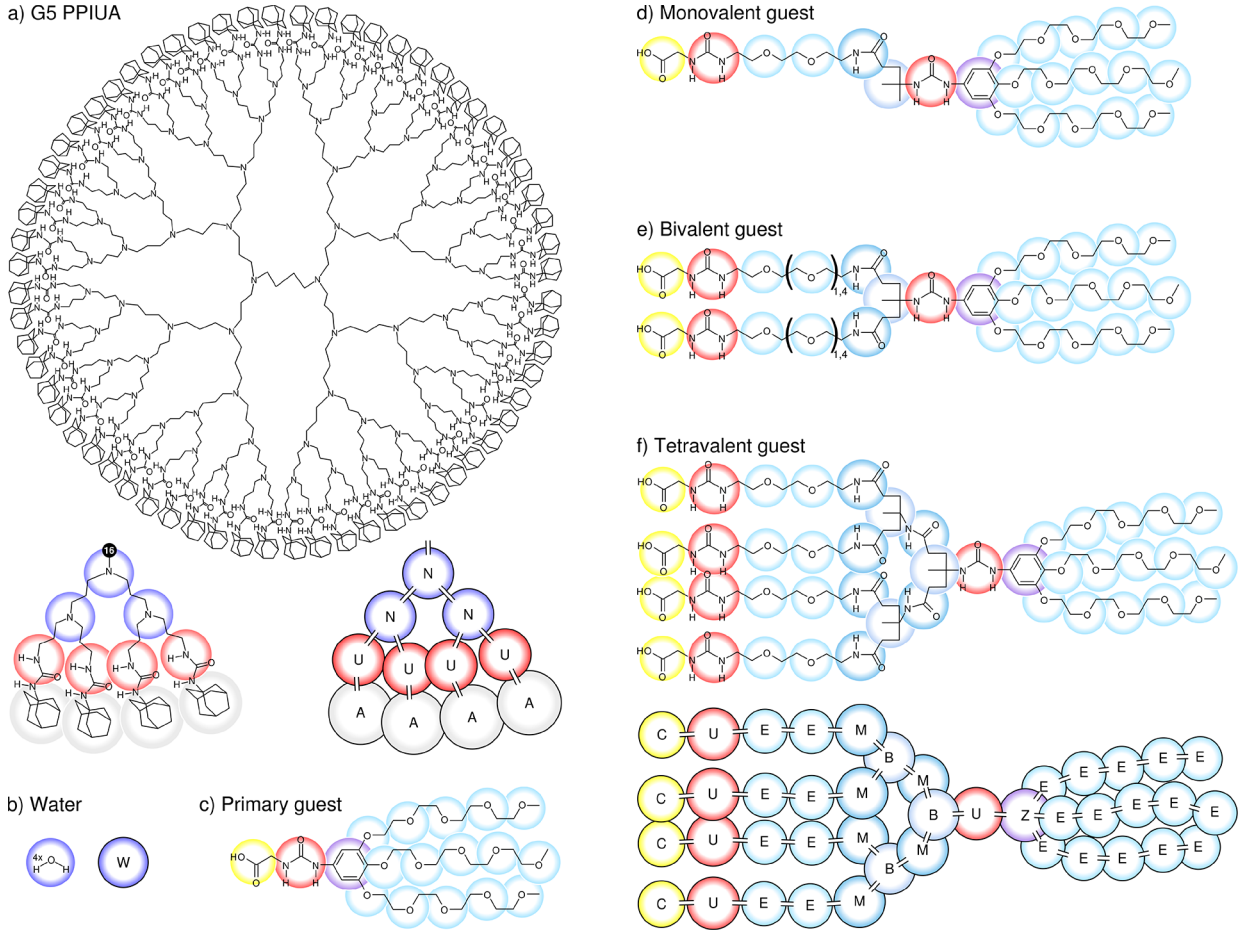

Figure 1. Two-dimensional representations of the molecules, showing the coarse-grained sites and the equivalent coarse-grained structures. (a) *G*5 PPIUA, the fifth-generation urea−adamantyl (U−A) decorated poly(propyleneimine) dendrimer made from trimethylamines (N). (b) Water particle (W) representing four water molecules. (c) Primary ureidoacetic acid guest. (d) Monovalent guest. (e) Bivalent guest. (f) Tetravalent guest. The multivalent guests may bind to the dendrimer with their headgroups containing an acetic acid (carboxylic acid, C) and urea moiety (U), each followed by a spacer of ethylene oxide (E). These are connected to a bifurcating part consisting of *N*-methylacetamide (M) and isobutane (B) which is linked to a hub made up of an urea and a benzene group (Z). The hub further holds three ethylene oxide tails. The ethylene oxide spacers are two moieties long, except for the elongated bivalent guests which contain three additional moieties per spacer.

Here, we study the aggregation of dendritic host−guest complexes as well as the host−guest interactions using molecular dynamics (MD) simulations for monovalent as well as multivalent guest compounds. Specifically, we consider the fifth-generation urea−adamantyl-terminated poly(propyleneimine) dendrimer (PPIUA, *G*5: DAB-dendr-(urea-adamantyl)$_{64}$, Figure 1a) in combination with mono-, bi-, and tetravalent ureidoacetic acid guests (Figure 1d−f). For this purpose we expand our coarse-grained (CG) PPIUA dendrimer model[18] with multivalent acetic acid guests. Simulations of dendrimers with guests have been reported previously.[19,20] They typically involve a dendrimer encapsulating small molecules[21−26] (a dendritic box[10]) or dendrimer−DNA/RNA coiling.[27−31] Though the latter could be considered as multivalent interactions between large polyelectrolytes, simulations of dendrimers with many small multivalent guests are novel. Moreover, this dendrimer−guest system provides a nice platform to investigate the multivalency effect on a small spherical object containing an abundance of receptors.

In the next section we describe the CG models of PPIUA and primary and multivalent guests as well as the simulation arrangements. This is followed by simulation results of macromolecular structure formation through self-assembly of patchy nanoparticles. Subsequently, we use the high temporal and spatial resolution of MD simulations to zoom in on the binding sites to uncover the ligand−receptor binding details. Next, we investigate the effect of multivalency by checking the concentration-dependent binding strength, the effective concentration of binding sites, and how the length of the spacer connecting the headgroups impacts binding. Finally, we show the benefit of multivalency through a competition between mono- and tetravalent guests.

2. MODEL

Previously, we have used fully atomistic MD simulations to determine the number of dendrimers present in spherical assemblies with a diameter of about 4 nm, as were observed using cryo-TEM imaging.[15] Assemblies ranging from 1 to 6 dendrimers were constructed and coated with 32 guests per dendrimer to obtain their hydrodynamic radii. Although chemically speaking association and dissociation of a guest to the dendrimer is fast—in chloroform equilibrium is reached within 2.4 ms,[15] the temporal resolution of ^{13}C NMR—to reproduce a statistically relevant number of these events using fully atomistic MD is impractical. The size and time scales

DOI: 10.1021/acs.macromol.8b02357
Macromolecules 2019, 52, 2778−2788

required are too large to follow dynamic interactions between host, guest, and solvent molecules in a reasonable amount of time. To simulate the host−guest complexation and complex aggregation in explicit solvent, we use a coarse-graining scheme, wherein roughly four heavy atoms are united to form a single particle. This reduces the computational cost significantly as fewer particles need to be considered and larger time steps can be applied as the higher frequency motions are removed. Moreover, because the CG system experiences less friction, the apparent dynamics are faster.[32]

We employ the coarse-grained PPIUA dendrimer and guest models illustrated in Figure 1. The dendrimer model was previously developed to examine the behavior of PPIUA and poly(propyleneimine) (PPI) dendrimers in water[18] and parametrized based on matching thermodynamic data (like in our lipid model[33−35]) and a Boltzmann inversion scheme on bond and angle distributions accumulated from atomistic simulations of *G*5 PPIUA. In this model all nonbonded interactions between groups of atoms, i.e., van der Waals and Coulombic, are described by a single Lennard-Jones potential between the coarse-grained particles they are represented by. This model corresponds well with atomistic simulations and experiments over a range of generations (*G*1 to *G*7). Furthermore, the *G*4 and *G*5 PPI models provided a clear concentration-dependent molecular picture in simulations of up to 1430 dendrimers in water from dilute to melt conditions and compared well with experimental SANS data.[36] It demonstrated that even at high concentrations each dendrimer remains a distinct entity and that structure factors computed using the approximations and assumptions experimenters need to employ start to diverge at rather low concentrations from structure factors derived directly from the simulation data.

Here, the dendrimer model is expanded with primary, mono-, bi-, and tetravalent ureidoacetic acid guest molecules applying the same modeling techniques as for the dendrimers, i.e., based on a combination of Boltzmann inversion of underlying atomistic simulations and thermodynamic data. To ensure the model displays the correct host−guest behavior, the competing interactions between carboxylic acid and amine (C---N) on one end and ethylene oxide tails and water (E---W) on the other were tuned to match the observed equilibrium in ^{1}H-DOSY NMR diffusion experiments. These show that at a primary guest concentration of 4.92×10^{-2} mol/L and a guest-to-host ratio of 64 the fraction of guest molecules bound to the dendrimers is ∼53%.[16] Details regarding parameter determination and the acquired bond, angle, and Lennard-Jones parameters are given in the Supporting Information section 1.

Unless explicitly noted otherwise, all simulations are performed using this coarse-grained model. The initial configuration of the simulations consist of either a single centered dendrimer or 16 dendrimers spread over the simulation box, with guests evenly distributed in explicit solvent. For lower concentrations guests were randomly pruned. These simulations were performed using our in-house-developed MD platform PumMa[37] under constant pressure (1 bar) and temperature (298 K) using Berendsen pressure and temperature coupling. With time steps of 24 fs, every 0.06 ns a configuration was saved for further analysis. Further simulation details are given in the Supporting Information section 2.1.

In the simulations we consider a headgroup being bound to the dendrimer if the carboxylic acid particle is within 0.7 nm of a tertiary amine, a distance at which no water particle fits in between. Guests are deemed bound if any headgroup is bound. Being unbound thus does not necessarily mean the guest is freely floating in the solvent. It may still be located at the dendrimer−water interface.

3. RESULTS AND DISCUSSION

3.1. Macromolecular Nanostructures. To investigate how the formation of macromolecular nanostructures through self-assembly of dynamic patchy nanoparticles is affected by the guest concentration, we simulate 16 dendrimers in a 2.56×10^4 nm^3 water box with a low guest concentration (24 tetravalent guests, 1.54×10^{-3} mol/L) and with a high guest concentration (300 tetravalent guests, 1.96×10^{-2} mol/L) for 480 ns. At the start the guests are distributed in the solvent (details available in Supporting Information section 2.1.1).

Figures 2a and 2b depict the aggregation states after 240 ns, i.e., halfway into the simulations, for the low and high guest concentrations, respectively. In the low concentration simulation the dendrimers form one large cluster (10 dendrimers) and two smaller ones. In the high concentration simulation five small clusters are present, although they appear quite bulky because of the associated guests. To investigate the aggregation as a function of time, we created clustering timelines (Figure 2c,e). These show that in the initial 60 ns there is little difference between both regimes; dendrimers coming into contact aggregate swiftly and the guests have not yet coated them. The subsequent 140 ns, aggregation is rare for the high concentration simulation, while it continues apace in the low concentration simulation. Eventually aggregation slows down because it takes time for the larger clusters to come into contact. At low guest concentration aggregation proceeds at approximately the same rate as in a control simulation without guests, showing that the guests are unable to impede aggregation. While aggregation is slower for the high guest concentration simulation, the outcome after 480 ns is similar for both simulations: two spherical assemblies, one containing the majority of the dendrimers and the other containing the rest.

The hypothesis put forward with the cryo-TEM experiments[16] that different guest concentrations lead to different aggregate structures via altered hydrophobic patches—e.g., two hydrophobic patches per dendrimer make for a dendrimer string while more patches build a network—could not be verified with these simulations as the high guest concentration simulation ultimately resulted in similar globular clusters as in the low guest concentration simulation. Rather, these clusters evoke an alternative experimentally observed result, namely, the globular *trapped core* structures[15,16] that were formed at a primary guest-to-host ratio of 32 irrespective of the guest concentration. Because of their dynamic nature, the guests are so mobile that while they do hinder aggregation some of the time, at other moments they leave parts of the dendrimer exposed. Once dendrimers come into contact at these hydrophobic patches, the guests simply continue to move out of their way, further increasing the binding surface. As the guests do not separate previously aggregated dendrimers, eventually the clusters become spherical as the guests do not impose otherwise. However, with enduring growth of a globular cluster, its volume keeps increasing more rapidly than its surface area, thus strengthening the guest coverage of the dendrimer−water interface and in turn limiting the expansion of dendrimer−dendrimer contacts. Other aggregate morphologies may thus be expected when larger numbers of

DOI: 10.1021/acs.macromol.8b02357
Macromolecules 2019, 52, 2778−2788

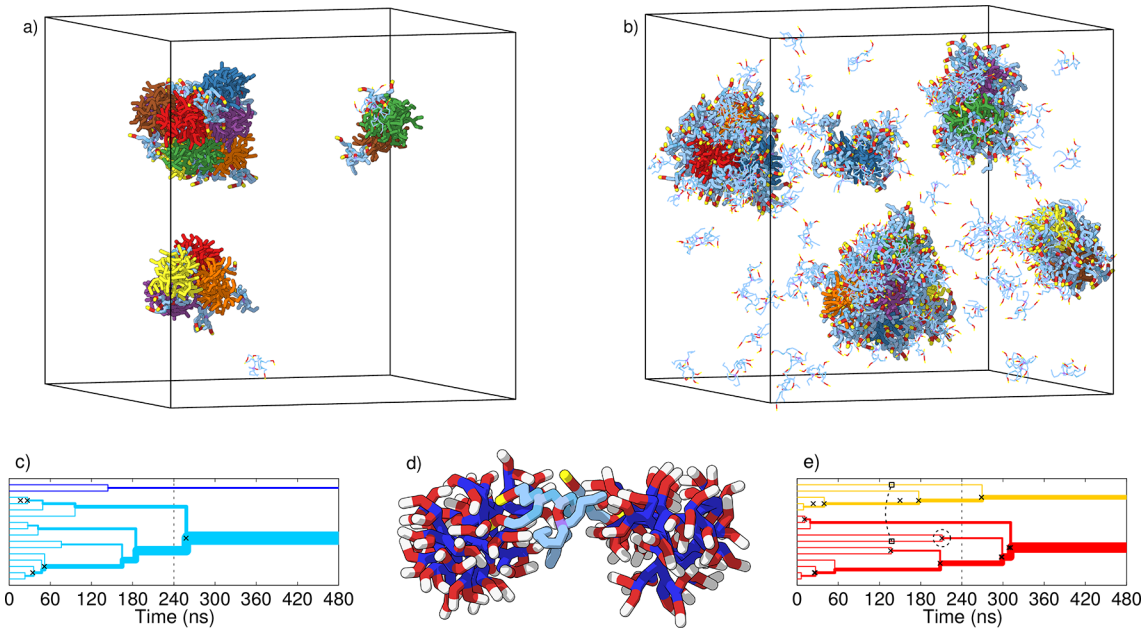

Figure 2. Aggregation of dendrimers and tetravalent guests. (a, b) Snapshots of the complexes formed halfway into the simulation (after 240 ns) for the low and high guest concentrations, respectively. Each dendrimer is colored distinctly, guests not bound to a dendrimer are drawn thinner, and water is omitted for clarity. (c, e) Timelines of the dendrimer aggregation for the low and high guest concentration simulations, respectively. Each line represents an aggregate, its width proportional to the number of incorporated dendrimers. Upon fusion of two aggregates, their lines are likewise merged. Guests bridging aggregates leading to fusion are marked with a cross. (d) Details showing a bridge, colored as in Figure 1. It is the instance marked with a dashed circle in (e) where a link is formed 0.3 ns before the two dendrimers aggregate, resulting in the rightmost cluster in (b). Not all bridges precede fusion; the dashed curve linking two lines in (e) represents such a fleeting connection.

dendrimers are present, requiring simulations increased in scope to be observed.

An interesting side effect of the tetravalent guests is their ability to bind to multiple dendrimers, effectively keeping otherwise separate dendrimer–guest complexes near (Figure 2d). Multiple times such a bridge formation precedes actual aggregation; other times the dendrimers separate despite the bridge. A similar bridging effect was exploited to create transient networks between dendrimers in chloroform by means of long linear chains with headgroups at both ends.[38]

3.2. Guest Binding Details. Having demonstrated the solubility effect the guests have on the dendrimers when bound, we now take a closer look at how they are bound using simulations with a single dendrimer in a 3007 nm^3 water box and 8 guests lasting 960 ns or 96 guests lasting 480 ns (simulation details are available in Supporting Information section 2.1.2).

Figure 3b shows a cross section of a dendrimer with a bound monovalent guest. Originally, the dendrimers were conceived to have discrete receptors acting as *pincers*:[40−42] The ends bifurcate at a tertiary amine, which is flanked by two ureas each capped by an adamantyl moiety. The guest headgroup was envisioned to bind to the amine with its carboxylic acid end in an acid–base electrostatic interaction, its urea would form hydrogen bonds with both ureas of the pincer, and the benzene ring would be matched by the adamantyl groups for a hydrophobic interaction. In practice any of these interactions may be present, but not all in the same pincer, as the headgroup is too large to fit.[39] Examples of typical interactions are depicted in the schematic of Figure 3a. In accordance with the schematic, in the CG simulations binding is more intricate than the pincer ideal suggests. The important host–guest interactions are present, just not limited to groups of one bifurcated branch. Additionally, the ethylene oxide tails are shown to project into the surrounding water.

To compare the binding under different guest conditions, we created radial monomer density profiles, which show the monomer density as a function of the distance from the dendrimer's center of mass (for the equation see Supporting Information section 3.1). The difference between bound mono-, bi-, and tetravalent guests was studied in a simulation with 8 guests present and fewer bound (Figure 3c). The dendrimer is unaffected by the change in guest valency. As only bound guests are taken into account in the profiles, the differences for the headgroups (C, U) beyond the dendrimer's periphery stem from additional unbound headgroups. All guests' carboxylic acid ends manage to penetrate toward the center of the dendrimer, followed by the urea particle. The hub (U, Z) represents the part where the tails originate. It is located near the periphery, although for the tetravalent guests it is shifted away from the center because of its larger connecting part (B, M).

Subsequently, the effect of saturation of a dendrimer with monovalent guests was investigated by adding an excess of 96 guests (Figure 3d). This leads the dendrimer to become swollen, while the adamantyl (A) distribution shifts from the center toward the perimeter with less back-folding ends on account of the first three generational branches being straighter. Whenever possible, the headgroups are forced a little toward the center of the dendrimer while the tails (Z, E) stick out into the solution. Thus, to accommodate more bound guests, each guest loses some freedom of movement and becomes increasingly stretched.

3.3. Multivalent Guest Concentrations. To investigate the degree of guest binding as a function of the concentration, we performed additional simulations of the single dendrimer

DOI: 10.1021/acs.macromol.8b02357
Macromolecules 2019, 52, 2778−2788

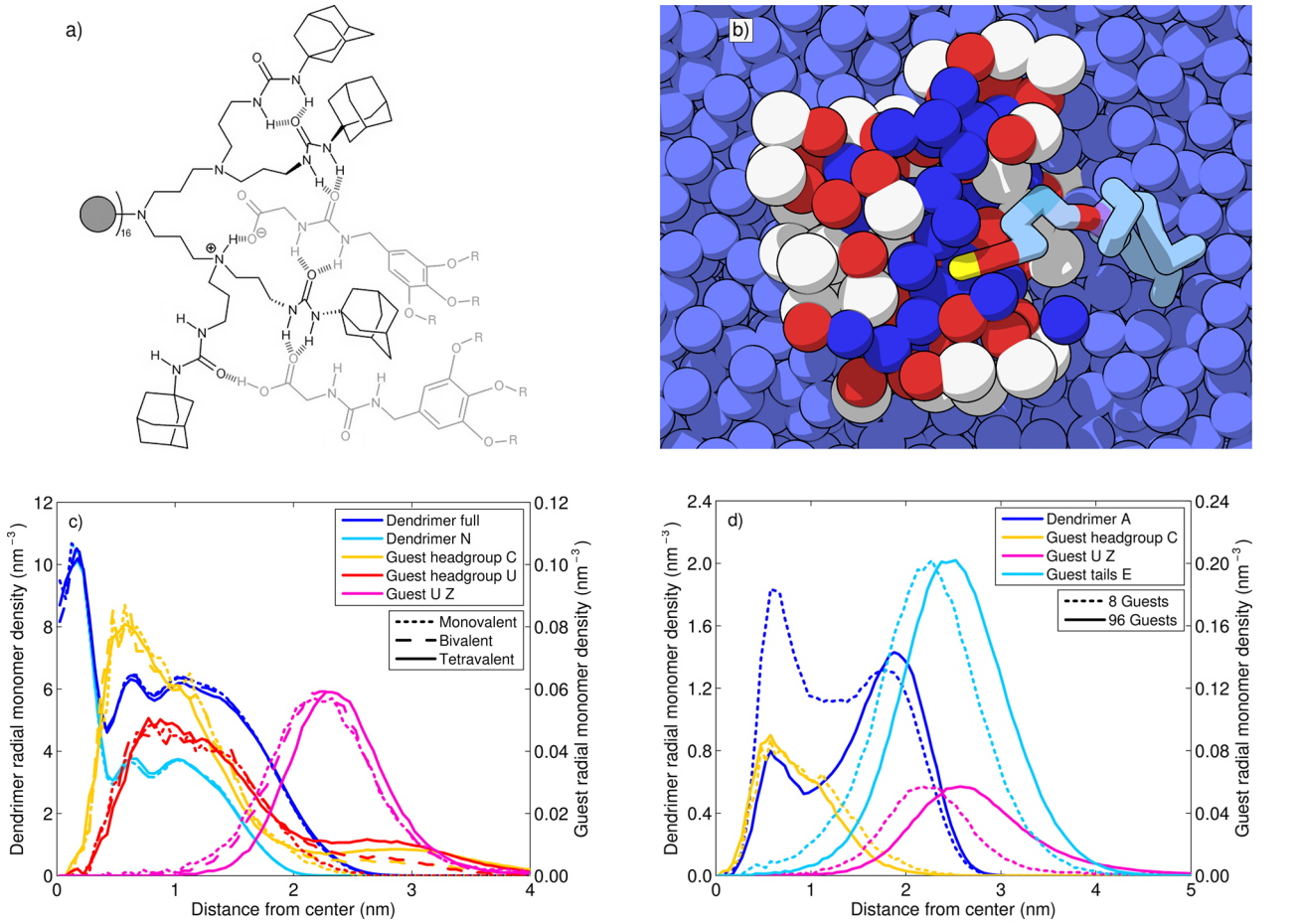

Figure 3. Binding of the guests to a dendrimer host. (a) Schematic of the predominant interaction modes of a PPIUA dendrimer with primary ureidoacetic acid guests adapted from Chang et al.[39] (b) A cross-sectional view of a simulated dendrimer with bound monovalent guest, colored as in Figure 1. (c) Radial monomer density profiles of a dendrimer with 8 mono-, bi-, or tetravalent guests. (d) Radial monomer density profiles of a dendrimer with 8 or 96 monovalent guests. In the density profiles only bound guests are considered. Guest curves are scaled to match the height of the curves from the 8 monovalent guests simulation to emphasize shape differences.

with numbers of guests varying between 1 and 96, where the simulations up to 8 guests lasted for 960 ns and those with more than 8 guests 480 ns. The average percentage of guests bound in these simulations, which characterizes the guest's binding strength, is shown in Figure 4a.

With few guests present, there clearly is increased binding achieved by multivalency. As the inset in Figure 4a shows, at low guest concentrations the bivalent guest binds 1.7 times as much as a monovalent one, and the tetravalent guest binds 3.3 times as much. Viewed another way, the two headgroups of the bivalent guest contribute 85% of the binding strength of the monovalent headgroup, and each of the tetravalent headgroups provides 82%. However, the benefit of multivalency is highly concentration dependent. The graph shows that with increasing guest concentrations the difference in binding percentage diminishes. At 80 guests (4.6×10^{-2} mol/L) only 15% is bound independent of their valency.

An alternative perspective is that by tying headgroups together their binding incidence is increased. A *tethering effect* increases headgroup binding as when one is bound the others are also near a binding site. Figure 4b shows that the number of headgroups bound as a function of the total number of headgroups present is rather independent of guest valency. Only at low guest numbers (fewer than 32 guests) more than 4 times as many tetravalent headgroups are bound than monovalent headgroups. The bivalent guests are worse off with a cutoff at fewer than 8 guests. Thus, from the perspective of a headgroup, when other headgroups are attached its relative binding performance improves only at low guest concentrations. At higher guest concentrations the competition for the binding sites by headgroups from free guests suffices to overcome the adjacency advantage of the tethered headgroups. In fact, surrounding the dendrimer, the concentration of tethered headgroups is indeed larger than the concentration of headgroups of free tetravalent guests in the simulations of up to 32 guests.

When a receptor changes binding affinity upon binding of a ligand, it is called cooperative binding. A well-known example is the positive cooperative binding of oxygen to hemoglobin. Upon binding of one oxygen molecule the three other binding sites become more accessible.[43] Though the dendrimer is not specifically designed to exhibit cooperative binding in this manner, we investigated its presence using the Hill equation[44]

$$\theta = \frac{1}{\left(\frac{G_{50}}{[G]}\right)^{n} + 1} \tag{1}$$

which describes the fraction of occupied binding sites (θ) as a function of the guest concentration ($[G]$) where G_{50} is the guest concentration producing half occupation. The Hill

DOI: 10.1021/acs.macromol.8b02357
Macromolecules 2019, 52, 2778−2788

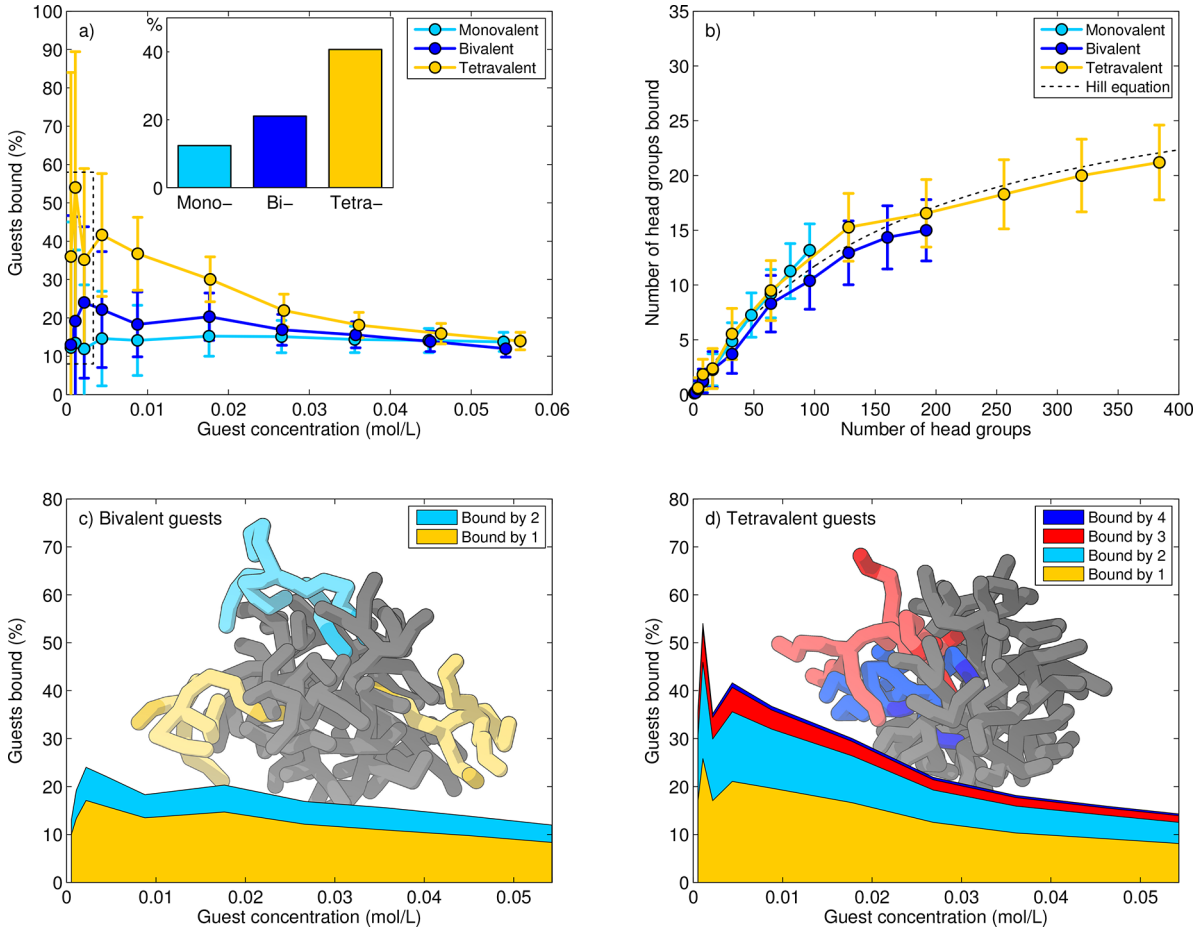

Figure 4. Guest concentration dependent host–guest binding. (a) Percentage of guests bound as a function of the guest concentration. Error bars indicate the variability throughout the simulation by showing the standard deviation around the mean. The bar plot inset shows the weighted average of the three lowest guest concentrations. (b) Number of headgroups bound as a function of the number of headgroups present, including a Hill equation fit to the tetravalent data for noncooperative binding with 32 binding sites. (c, d) Reiteration of (a) with the curves split into stacked areas indicating the number of headgroups bound for the bivalent and tetravalent guests, respectively. Background illustrations are snapshots of a dendrimer with guests colored according to the number of headgroups bound; headgroups are darkened for clarity.

coefficient (n) varies with the kind of cooperativity, i.e., positively ($n > 1$) or negatively cooperative ($n < 1$). The tetravalent headgroup data are nicely fit with $n = 1$ (Figure 4b), i.e., assuming completely independent binding, confirming the noncooperativity. The dendrimer's affinity for headgroups thus does not measurably change upon binding of headgroups.

Finally, the stacked area graphs in Figure 4c,d show the binding stoichiometry, i.e., the number of headgroups responsible for the binding of the guests. Most of the bound guests are only held by a single headgroup. In the case of the bivalent guests, roughly 72% of the bound guests are bound by a single headgroup only. The tetravalent guests are more frequently bound by multiple headgroups. Yet the fraction bound with all four headgroups is almost negligible, and still approximately half are bound by a single one.

The figures all indicate that with increased guest concentration the returns for guest binding diminish. This raises the question how many headgroups the dendrimer can accommodate before it is saturated. The fifth-generation PPIUA dendrimer has 32 pincers, but the actual binding sites are ill-defined. In a series of reference simulations with very strong binding guests (i.e., a 66% stronger headgroup–amine interaction) in systems up to 32 headgroups all headgroups were bound all the time regardless of guest valency. Moreover, with 64 tetravalent guests on average 58 headgroups were bound, demonstrating that there are no steric reasons for having fewer than 32 headgroups bound.

Collectively, these results show that although the dendrimer–guest binding is noncooperative, at low guest concentrations the guest binding does increase with guest valency and that although the dendrimer provides plenty of space for headgroups, most multivalent guests leave part of their headgroups unbound.

3.4. Effective Concentration. In the previous section we observed that when bivalent guests are bound to the dendrimer, frequently one headgroup has not found a binding site. We now further examine how such a pair of headgroups connected by a flexible linker fares. In particular, we analyze the distances between the headgroups discerning the cases where both headgroups are free, one is bound, or both are bound (Figure 5b). The end-to-end headgroup distributions from all bivalent guest simulations combined (2401851 samples) are shown in Figure 5a.

The unbound guests display a wide ranging end-to-end distribution, from headgroups touching to totally spread apart, with an average end-to-end distance of 1.7 nm. To further validate the free guest behavior, we compare the CG simulations with a separate 20 ns fully atomistic simulation

DOI: 10.1021/acs.macromol.8b02357
Macromolecules 2019, 52, 2778–2788

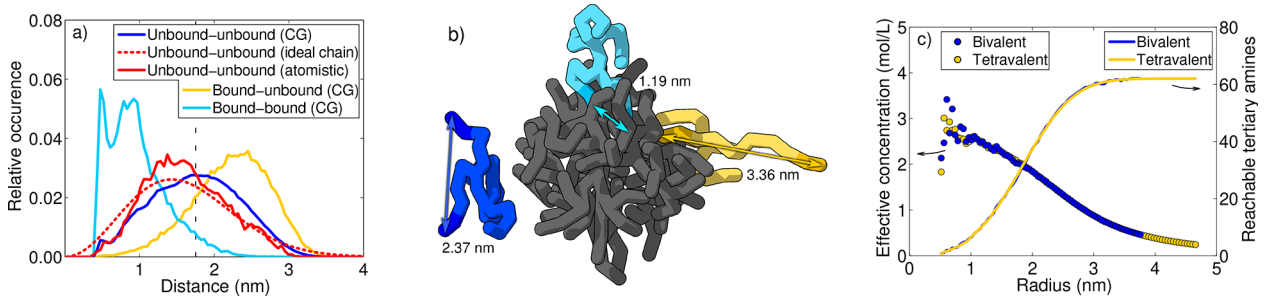

Figure 5. Connected headgroup pairs. (a) Normalized distributions of the CG headgroup−headgroup distances of the bivalent guests categorized by the number of headgroups bound. Also present are atomistic simulation and ideal chain model distributions of the free guest. The model is fitted to the average end-to-end distance (1.7 nm, dashed line) of the CG simulations. (b) A snapshot of a dendrimer with 3 bivalent guests illustrating the different binding states colored as in (c). Arrows highlight the headgroup−headgroup distances. (d) The number of tertiary amines (right *y*-axis) found within a sphere centered at the anchoring headgroup of a semibound guest with the end-to-end distance as its radius and the concentration ($C_{\mathrm{eff,max}}$, left *y*-axis) of tertiary amines within said sphere.

of a solvated bivalent guest (simulation details in the Supporting Information section 2.2.1) and with the freely jointed ideal chain[45,46] model. According to this model, which considers a polymer chain sufficiently long to be characterized as a random walk of N segments of length l, the distribution of the end-to-end distances (r) is given by

$$P(r) = 4\pi r^2 \left(\frac{3}{2\pi N l^2}\right)^{3/2} \mathrm{e}^{-3r^2/2Nl^2} \tag{2}$$

with an average end-to-end distance of $\sqrt{Nl^2}$. The atomistic simulation's distribution consisting of 20000 samples of the distance between carboxylic acid ends is obviously not as smooth. The observed mismatch with the ideal chain distribution stems from the guest's chain being too short (34 bonds between ends) to warrant the model's usage. Such mismatch was earlier shown for alkane chains of 43 bonds, while it vanished with 99 bonds.[47] Also, due to excluded volume effects, the CG ends cannot come nearer than 0.4 nm. Nevertheless, comparing the CG free guests with their atomistic counterpart shows their end-to-end distributions breadth to be quite similar. The agreement with the ideal chain model underlines that despite the presence of other guests and the dendrimer, the headgroups of the free bivalent guest actually experience free movement in the solvent. The chains consisting of headgroups, spacers, and connectors are flexible and sufficiently water-soluble. Remarkably, when the guests are fully bound, their headgroups are usually quite close together. Even though the guests are flexible and can span sites 3 nm apart, the majority of the headgroups end up bound near each other. The first peak, for end-groups in direct contact, contains 21% of the fully bound guests. Only 4% are found further than 1.7 nm apart. Conversely, for the semibound guests the distribution is shifted to the right as free ends coming near a bound end have a tendency to become bound themselves. Finally, despite that the tetravalent guest effectively has six headgroup pairs, their end-to-end distributions are quite similar to these bivalent ones, particularly when both ends are bound (Supporting Information section 3.2).

When one headgroup of a multivalent guest is bound to a host with multiple binding sites, the binding chance of the unbound headgroups depends on the number of unoccupied binding sites within reach. This quantity, used in certain binding models, is known as the effective concentration:[48]

$$C_{\mathrm{eff,max}} = \frac{n_{\mathrm{H}}(L)}{N_{\mathrm{A}} V(L)} \tag{3}$$

That is, the concentration of accessible host sites (n_{H}) in the volume (V) that can be probed by a headgroup tethered with a linker of length L, with N_{A} Avogadro's number. The "max" subscript denotes occupied host sites are also deemed available.

In the simulations, we can directly derive the instantaneous effective concentration by observing the distance between bound and unbound ends and counting the number of host sites that lie within the sphere originating at the bound end with that distance as its radius. Then $C_{\mathrm{eff,max}}$ is the concentration of tertiary amines within the volume enclosed by that sphere. From Figure 5c it is clear that as the bivalent guest's total chain length is larger than 3 nm, when one end is bound, in principle the whole dendrimer is within reach of the free end. Thus, while the tetravalent guest has a 20% larger reach it attains the same number of reachable sites and the $C_{\mathrm{eff,max}}$ is similar, except at small distances where irregularities are magnified. Precisely because there the concentration of possible binding sites is large, few data points are available for semibound distances that small. Our calculated $C_{\mathrm{eff,max}}$ is high in comparison with literature values of other systems (e.g., 0.8 mol/L[48]). This is mainly due to the flexible and open nature of the receptor (Figure 3): it is not just a surface layer of binding sites; instead, there is a large assembly of binding sites in the dendrimer interior that are all accessible. Additionally, the accessibility of the binding sites is overestimated as it is unlikely that sites on the far side of the dendrimer are actually preferred over nearby sites.

3.5. Alternative Spacer Length. To investigate the effect of the headgroup−headgroup chain length on the binding of the multivalent guests, elongated bivalent guests were created with five instead of two ethylene oxide spacer moieties (Figure 1e). The molecule's total chain length was thus increased from 4.0 to 6.2 nm. This elongated guest was simulated at various concentrations together with a single dendrimer, following the same procedure as the regular bivalent guest simulations of section 3.3 (simulation details in Supporting Information section 2.1.2).

As shown in Figure 6a, the elongated spacers increase the binding by 50 percent. A first hypothesis for this enhanced binding is that because the chain is longer, each headgroup may find an optimal binding site without having to reckon with the headgroup at the other end. If the elongated guest is better

DOI: 10.1021/acs.macromol.8b02357
Macromolecules 2019, 52, 2778−2788

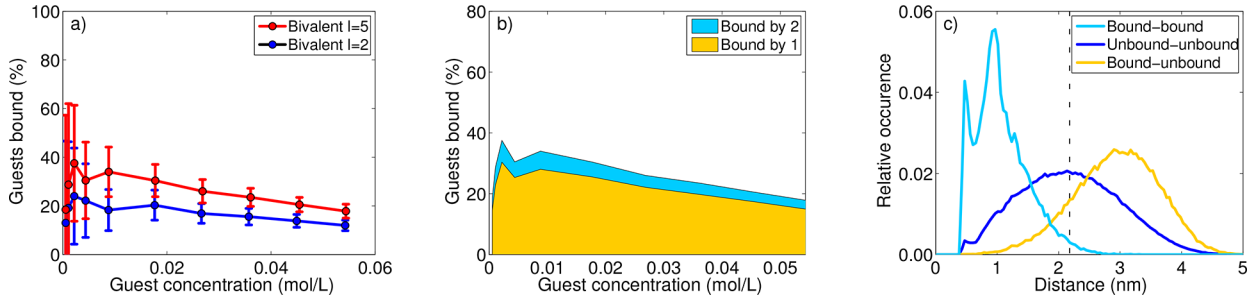

Figure 6. Elongated bivalent guests. (a) Percentage of guests bound as a function of the guest concentration. (b) Percentage bound shown in a stacked area graph. (c) Normalized end-to-end distance distributions of the elongated bivalent guests categorized by the number of headgroups bound. The average free end-to-end distance (dashed line) is 2.1 nm.

in this regard, then one would expect that it has the higher percentage of doubly bound guests, because each headgroup is held longer. Comparing Figures 4c and 6b this proves not the case. Quite the contrary: whereas 28% of the regular bound guests was fully bound, this holds for only 17% of the bound elongated ones. In simulations with up to 16 guests, the absolute number of fully bound guests are approximately the same. At higher concentrations the regular guest is more fully bound. Examining the radial monomer densities (Supporting Information section 3.3) shows the elongated guest's headgroup particles (C, U) to be similarly distributed as in Figure 3c, indicating no physical change in binding. As expected, the rest of the molecule is situated further from the dendrimer center of mass.

An alternative hypothesis for increased binding is that because the end-to-end distance is longer, more of the dendrimer is within reach once the first headgroup is bound. While the premise is true, it does not lead to increased binding. As we have seen in the previous section, the longer tether also probes more of the environment; thus, it rather lowers the effective concentration. Moreover the regular bivalent guest is already sufficiently long to theoretically span the whole dendrimer. All amines lie within 3 nm from a binding site (Figure 5c) while the bivalent guest can extend a bit further (Figure 5a). Besides, Figure 6c shows that despite the longer spacer, the bound headgroups still prefer to bind close together. Although in theory the most effective bivalent guest exactly fits two binding sites without a longer than necessary spacer and is rigid rather than flexible, as the excess chain only adds more unfavorable conformations and thus increases the entropic cost of association,[1] several experimental studies on multivalent binding involving functional guests connected by long flexible spacers[2,49,50] have also shown that in practice these entropic concerns are not insurmountable.

Ultimately, larger guests are simply more likely to encounter the dendrimer. Even though the headgroup concentration for both guest variants is the same, the guests consist of more than the parts that prefer to bind to the binding sites. The other parts do come into contact with the dendrimer and cause the guest to linger there through aspecific interactions because their solubility is not absolute. The extended spacers increase the average end-to-end distance between headgroups of the free guests from 1.7 to 2.1 nm (Figures 5a and 6c), increasing their chance to encounter the dendrimer and remain there. These results also confirm the picture Weber et al.[51] painted using a Markov chain Monte Carlo model of weak binding ligands attached with flexible spacers to a slow moving particle: The complex is strong because dissociated ligands can rebind before the particle diffuses away. The lingering effect is also visible in Figure 2b, where many unbound, line-drawn, tetravalent guests are free in solution but roughly equal as many are in the vicinity of the dendrimers. In conclusion, the spacer contributes more to the guest than just additional length.

3.6. Competition between Guest Types. The observed host−guest systems exhibit striking differences in the binding strength at low guest concentrations (<0.01 mol/L), but at high concentrations (>0.04 mol/L) the percentage bound drops to 14% for all multivalent types (Figure 4a). This should not suggest that there is no difference in binding strength between the guest types at these concentrations, but rather that the binding sites begin to fail to optimally accommodate the larger number of guests. To investigate whether tetravalent guests continue to bind better than monovalent guests at high concentrations, we let them compete for binding space on the dendrimer.

For this experiment, simulations were performed of a single dendrimer with equal numbers of mono- and tetravalent guests in explicit water. For each guest concentration two simulations were performed: one starting with the dendrimer covered in monovalent guests and the tetravalent guests randomly distributed through the solvent and another with the guest types swapped (for simulation details see Supporting Information section 2.1.3). These disparate starting positions were chosen to test the adequacy of our equilibration time, for if these disparate simulations produce similar binding percentages, then any random starting distribution will as well.

In the simulations the guests exchange between the bound and unbound states, setting a new equilibrium with a new ratio of tetravalent and monovalent guests bound to the dendrimer. Figure 7a shows the percentages of bound monovalent and tetravalent guests for both simulations with 20 guests of each type as a function of time. For each guest type the average bound percentage converges to a single value within the standard equilibration time of 90 ns, demonstrating the latter is sufficiently long. On average 2.65 monovalent and 6.85 tetravalent guests are bound to the dendrimer. Tetravalent guests thus indeed also bind better at high concentration. Figure 7b provides an impression of such an average.

Comparing the previous unmixed simulations with simulations containing a range of competing guests (2, 5, 10, 20, 30, and 40 each; Figure 7c) shows there is little difference at low guest numbers. As an abundance of binding sites is available, both guest types can work independently of each other, thus yielding fractions of guests bound similar to the unmixed simulations. However, when the availability of binding sites

DOI: 10.1021/acs.macromol.8b02357
Macromolecules 2019, 52, 2778−2788

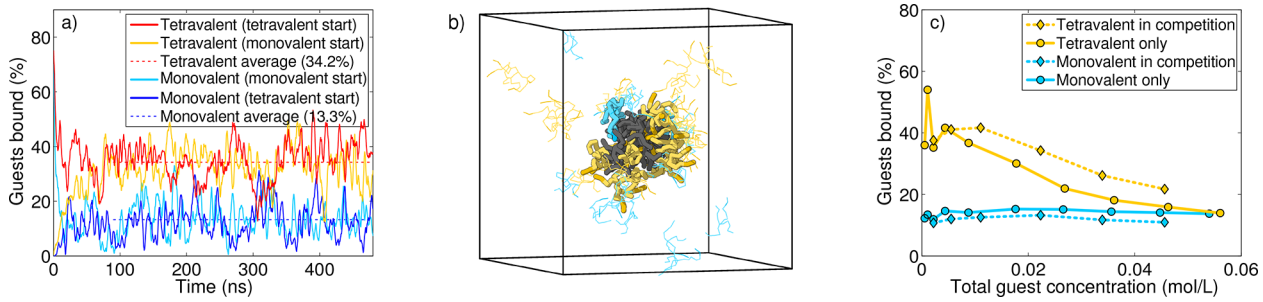

Figure 7. Competition between mono- and tetravalent guests binding to a dendrimer. (a) Percentage of monovalent and tetravalent guests bound to the dendrimer as a function of time for two simulations: one starting with 20 monovalent guests bound to the dendrimer and 20 tetravalent guests dispersed in the surrounding solvent, the other vice versa. Average bound percentages are shown as dashed lines. For clarity the curves are smoothed with a 3 ns moving average window. (b) Snapshot from the simulation that started with 20 bound monovalent guests featuring a dendrimer with the average number of monovalent (3) and tetravalent (7) guests bound (479.2 ns). (c) Competition shown as percentage of guests bound as a function of the guest concentration, averaged from two starting simulations for each data point. The unmixed values are from Figure 4a.

becomes an issue, the stronger binding tetravalent guest has a clear advantage over the monovalent guest and does bind relatively more.

The strong binding of multivalent guests is confirmed by competition experiments of trivalent vancomycin hosts and D-alanine−D-alanine guests in trivalent and monovalent variants.[52] The trivalent−trivalent host−guest complex is very stable with an estimated half-life of 200 days.[2] Only by adding over 3900 monovalent DADA guests for every trivalent one could the equilibrium be shifted so that just 60% of the complex remained within 45 min.

4. CONCLUSION

To investigate multivalent dendritic host−guest interactions as well as the aggregation of their complexes into macromolecular nanostructures, we expanded our coarse-grained urea−adamantyl-terminated poly(propyleneimine) dendrimer model to include multivalent ureidoacetic acid guests. The host−guest interactions were tuned to experimental values.

The first experiment involved the formation of macromolecular nanostructures through aggregation of the host−guest complexes. As the noncovalently bound guests lend their solubility to the otherwise hydrophobic dendrimers, these complexes serve as dynamic patchy nanoparticles. Hereby the guest concentration determines the coverage into hydrophilic and hydrophobic domains and in turn the self-assembly. The simulations, composed of 16 fifth-generation dendrimers with tetravalent guests at a 1.5- or 19-fold guest-to-host ratio, corroborated that the presence of more guests slows down the dendrimer self-assembly. However, the continual dissociation and association of guests ultimately resulted in spherical aggregates independent of the host−guest ratio. Moreover, the simulations showed that the multivalent guests not only solubilize dendrimer aggregates but also may keep separate aggregates close together by establishing a bridge between them.

The other simulations concern a single dendrimer with a range of guest concentrations. The way guests' headgroups are physically bound to the dendrimer is the same for the mono-, bi-, and tetravalent guests: the receptor does not conform to the pincer ideal; rather, the carboxylic acid−tertiary amine and urea−urea interactions readily occur with different branches of the dendrimer. When an excess of monovalent guests is present, the guests become stretched to accommodate additional guests.

At low guest concentrations, the multivalency effect is clear: tetravalent guests bind relatively more than bivalent ones, which in turn bind more than monovalent ones. Headgroups united into multivalent guests are bound more often, as when the first is bound, the others are also near binding sites. This adjacency advantage diminishes with higher guest concentrations: with over 32 guests in the simulation box, the concentration of unbound guests' headgroups surrounding the dendrimer exceeds the concentration of tethered headgroups. Indeed, only 28% of the bivalent guests are fully bound and tetravalent guests rarely have all four headgroups bound, yet approximately half are bound by multiple headgroups. Despite the abundance of binding sites, these headgroups tend to bind in close proximity: only 4% is bound further apart than the free guest's average end-to-end distance.

Using the semibound guests, we measured the effective concentration; i.e., the concentration of accessible host sites in the volume that can be probed by the tethered headgroups. The simulations reinforce that while these multivalent guests' chains are long enough to reach all the dendrimer's tertiary amines, for the highest $C_{\mathrm{eff,max}}$ the end-to-end distance should be small. Nevertheless, elongation of the chain by 55% enhances guest binding, as it raises the chance for free guests to encounter the dendrimer and increases lingering of dissociated headgroups in the periphery, thus promoting rebinding.

At high guest concentrations the dendrimer becomes saturated with bound headgroups regardless of the guest valency, thus diminishing the effect of multivalency. Nevertheless, when the monovalent and tetravalent guests are put in direct competition for binding sites, the multivalent guests displace the monovalent guests from the dendrimer, thus reaffirming the increased binding power provided by multivalency also at high concentration.

In the current model, for computational efficiency, electrostatic and van der Waals interactions were integrated into the Lennard-Jones potentials. Other coarse-graining strategies apply electrostatic interactions with a similar short-range cutoff[53] or even apply long-range electrostatics with particle mesh Ewald summation.[54] Given the importance of the acid−base interactions for host−guest binding it could be advantageous to treat the Coulombic interactions in more detail in future work.

DOI: 10.1021/acs.macromol.8b02357
Macromolecules 2019, 52, 2778−2788

This study illustrates how computer simulations aid in the design of functional multivalent host−guest systems. All together, the results show the enhancing effect of multivalency on guest binding over a full concentration range. Although these coarse-grained molecular dynamics simulations focused on a specific dendrimer with compatible multivalent guests, we expect these findings to be generally applicable to other multivalent host−guest systems, dendritic or otherwise.

■ ASSOCIATED CONTENT

Supporting Information

The Supporting Information is available free of charge on the ACS Publications website at DOI: 10.1021/acs.macromol.8b02357.

Model creation details, atomistic and CG simulation parameters, radial monomer density equation, tetravalent guest end-to-end distributions, and elongated guest radial monomer densities (PDF)

■ AUTHOR INFORMATION

Corresponding Author

*E-mail: a.j.markvoort@tue.nl.

ORCID

Albert J. Markvoort: 0000-0001-6025-9557

Notes

The authors declare no competing financial interest.

■ ACKNOWLEDGMENTS

The authors thank Prof. E. W. Meijer for his support.

■ REFERENCES

(1) Mammen, M.; Choi, S.-K.; Whitesides, G. M. Polyvalent interactions in biological systems: Implications for design and use of multivalent ligands and inhibitors. *Angew. Chem., Int. Ed.* **1998**, *37*, 2754−2794.

(2) Mulder, A.; Huskens, J.; Reinhoudt, D. N. Multivalency in supramolecular chemistry and nanofabrication. *Org. Biomol. Chem.* **2004**, *2*, 3409−3424.

(3) Badjić, J. D.; Nelson, A.; Cantrill, S. J.; Turnbull, W. B.; Stoddart, J. F. Multivalency and cooperativity in supramolecular chemistry. *Acc. Chem. Res.* **2005**, *38*, 723−732.

(4) Fasting, C.; Schalley, C. A.; Weber, M.; Seitz, O.; Hecht, S.; Koksch, B.; Dernedde, J.; Graf, C.; Knapp, E.-W.; Haag, R. Multivalency as a chemical organization and action principle. *Angew. Chem., Int. Ed.* **2012**, *51*, 10472−10498.

(5) Matthews, O. A.; Shipway, A. N.; Stoddart, J. F. Dendrimers−Branching out from curiosities into new technologies. *Prog. Polym. Sci.* **1998**, *23*, 1−56.

(6) Astruc, D.; Boisselier, E.; Ornelas, C. Dendrimers designed for functions: From physical, photophysical, and supramolecular properties to applications in sensing, catalysis, molecular electronics, photonics, and nanomedicine. *Chem. Rev.* **2010**, *110*, 1857−1959.

(7) Bosman, A. W.; Janssen, H. M.; Meijer, E. W. About dendrimers: Structure, physical properties, and applications. *Chem. Rev.* **1999**, *99*, 1665−1688.

(8) Tekade, R. K.; Kumar, P. V.; Jain, N. K. Dendrimers in oncology: An expanding horizon. *Chem. Rev.* **2009**, *109*, 49−87.

(9) Villaraza, A. J. L.; Bumb, A.; Brechbiel, M. W. Macromolecules, dendrimers, and nanomaterials in magnetic resonance imaging: The interplay between size, function, and pharmacokinetics. *Chem. Rev.* **2010**, *110*, 2921−2959.

(10) Jansen, J. F. G. A.; de Brabander-van den Berg, E. M. M.; Meijer, E. W. Encapsulation of guest molecules into a dendritic box. *Science* **1994**, *266*, 1226−1229.

(11) Mignani, S.; Rodrigues, J.; Tomas, H.; Roy, R.; Shi, X.; Majoral, J.-P. Bench-to-bedside translation of dendrimers: Reality or utopia? A concise analysis. *Adv. Drug Delivery Rev.* **2018**, *136-137*, 73.

(12) Kabanov, V. A.; Sergeyev, V. G.; Pyshkina, O. A.; Zinchenko, A. A.; Zezin, A. B.; Joosten, J. G. H.; Brackman, J.; Yoshikawa, K. Interpolyelectrolyte complexes formed by DNA and Astramol poly(propylene imine) dendrimers. *Macromolecules* **2000**, *33*, 9587−9593.

(13) Smith, D. K.; Hirst, A. R.; Love, C. S.; Hardy, J. G.; Brignell, S. V.; Huang, B. Self-assembly using dendritic building blocks−Towards controllable nanomaterials. *Prog. Polym. Sci.* **2005**, *30*, 220−293.

(14) Broeren, M. A. C.; Linhardt, J. G.; Malda, H.; de Waal, B. F. M.; Versteegen, R. M.; Meijer, J. T.; Lowik, D. W. P. M.; van Hest, J. C. M.; van Genderen, M. H. P.; Meijer, E. W. Noncovalent synthesis of supramolecular dendritic architectures in water. *J. Polym. Sci., Part A: Polym. Chem.* **2005**, *43*, 6431−6437.

(15) Hermans, T. M.; Broeren, M. A. C.; Gomopoulos, N.; Smeijers, A. F.; Mezari, B.; van Leeuwen, E. N. M.; Vos, M. R. J.; Magusin, P. C. M. M.; Hilbers, P. A. J.; van Genderen, M. H. P.; Sommerdijk, N. A. J. M.; Fytas, G.; Meijer, E. W. Stepwise noncovalent synthesis leading to dendrimer-based assemblies in water. *J. Am. Chem. Soc.* **2007**, *129*, 15631−15638.

(16) Hermans, T. M.; Broeren, M. A. C.; Gomopoulos, N.; van der Schoot, P.; van Genderen, M. H. P.; Sommerdijk, N. A. J. M.; Fytas, G.; Meijer, E. W. Self-assembly of soft nanoparticles with tunable patchiness. *Nat. Nanotechnol.* **2009**, *4*, 721−726.

(17) Glotzer, S. C.; Solomon, M. J. Anisotropy of building blocks and their assembly into complex structures. *Nat. Mater.* **2007**, *6*, 557−562.

(18) Smeijers, A. F.; Markvoort, A. J.; Pieterse, K.; Hilbers, P. A. J. Coarse-grained modelling of urea-adamantyl functionalized poly(propylene imine) dendrimers. *Mol. Simul.* **2016**, *42*, 882−895.

(19) Martinho, N.; Florindo, H.; Silva, L.; Brocchini, S.; Zloh, M.; Barata, T. Molecular modeling to study dendrimers for biomedical applications. *Molecules* **2014**, *19*, 20424−20467.

(20) Ramezanpour, M.; Leung, S. S. W.; Delgado-Magnero, K. H.; Bashe, B. Y. M.; Thewalt, J.; Tieleman, D. P. Computational and experimental approaches for investigating nanoparticle-based drug delivery systems. *Biochim. Biophys. Acta, Biomembr.* **2016**, *1858*, 1688−1709.

(21) Miklis, P.; Çağin, T.; Goddard, W. A., III Dynamics of Bengal Rose encapsulated in the Meijer dendrimer box. *J. Am. Chem. Soc.* **1997**, *119*, 7458−7462.

(22) Teobaldi, G.; Zerbetto, F. Molecular dynamics of a dendrimer-dye guest-host system. *J. Am. Chem. Soc.* **2003**, *125*, 7388−7393.

(23) Tanis, I.; Karatasos, K. Association of a weakly acidic anti-inflammatory drug (Ibuprofen) with a poly(amidoamine) dendrimer as studied by molecular dynamics simulations. *J. Phys. Chem. B* **2009**, *113*, 10984−10993.

(24) DeFever, R. S.; Sarupria, S. Association of small aromatic molecules with PAMAM dendrimers. *Phys. Chem. Chem. Phys.* **2015**, *17*, 29548−29557.

(25) Jain, V.; Maiti, P. K.; Bharatam, P. V. Atomic level insights into realistic molecular models of dendrimer-drug complexes through MD simulations. *J. Chem. Phys.* **2016**, *145*, 124902.

(26) Badalkhani-Khamseh, F.; Ebrahim-Habibi, A.; Hadipour, N. L. Atomistic computer simulations on multi-loaded PAMAM dendrimers: A comparison of amine- and hydroxyl-terminated dendrimers. *J. Comput.-Aided Mol. Des.* **2017**, *31*, 1097−1111.

(27) Lyulin, S. V.; Vattulainen, I.; Gurtovenko, A. A. Complexes comprised of charged dendrimers, linear polyelectrolytes, and counterions: Insight through coarse-grained molecular dynamics simulations. *Macromolecules* **2008**, *41*, 4961−4968.

(28) Pavan, G. M.; Albertazzi, L.; Danani, A. Ability to adapt: Different generations of PAMAM dendrimers show different behaviors in binding siRNA. *J. Phys. Chem. B* **2010**, *114*, 2667−2675.

(29) Vasumathi, V.; Maiti, P. K. Complexation of siRNA with dendrimer: A molecular modeling approach. *Macromolecules* **2010**, *43*, 8264−8274.

DOI: 10.1021/acs.macromol.8b02357
Macromolecules 2019, 52, 2778−2788

(30) Nandy, B.; Maiti, P. K. DNA compaction by a dendrimer. *J. Phys. Chem. B* **2011**, *115*, 217−230.
(31) Yu, S.; Larson, R. G. Monte-Carlo simulations of PAMAM dendrimer-DNA interactions. *Soft Matter* **2014**, *10*, 5325−5336.
(32) Markvoort, A. J. In *Computational Methods in Catalysis and Materials Science: An Introduction for Scientists and Engineers*; van Santen, R. A., Sautet, P., Eds.; Wiley: Weinheim, 2009; Chapter 8, pp 151−166.
(33) Smeijers, A. F.; Markvoort, A. J.; Pieterse, K.; Hilbers, P. A. J. A detailed look at vesicle fusion. *J. Phys. Chem. B* **2006**, *110*, 13212−13219.
(34) Markvoort, A. J.; Spijker, P.; Smeijers, A. F.; Pieterse, K.; van Santen, R. A.; Hilbers, P. A. J. Vesicle deformation by draining: Geometrical and topological shape changes. *J. Phys. Chem. B* **2009**, *113*, 8731−8737.
(35) van Hoof, B.; Markvoort, A. J.; van Santen, R. A.; Hilbers, P. A. J. Molecular simulation of protein encapsulation in vesicle formation. *J. Phys. Chem. B* **2014**, *118*, 3346−3354.
(36) Smeijers, A. F.; Markvoort, A. J.; Pieterse, K.; Hilbers, P. A. J. Coarse-grained simulations of poly(propylene imine) dendrimers in solution. *J. Chem. Phys.* **2016**, *144*, 074903.
(37) Markvoort, A. J.; Pieterse, K.; Steijaert, M. N.; Spijker, P.; Hilbers, P. A. J. The bilayer-vesicle transition is entropy driven. *J. Phys. Chem. B* **2005**, *109*, 22649−22654.
(38) Versteegen, R. M.; van Beek, D. J. M.; Sijbesma, R. P.; Vlassopoulos, D.; Fytas, G.; Meijer, E. W. Dendrimer-based transient supramolecular networks. *J. Am. Chem. Soc.* **2005**, *127*, 13862−13868.
(39) Chang, T.; Pieterse, K.; Broeren, M. A. C.; Kooijman, H.; Spek, A. L.; Hilbers, P. A. J.; Meijer, E. W. Structural elucidation of dendritic host-guest complexes by X-ray crystallography and molecular dynamics simulations. *Chem. - Eur. J.* **2007**, *13*, 7883−7889.
(40) Baars, M. W. P. L.; Karlsson, A. J.; Sorokin, V.; de Waal, B. F. W.; Meijer, E. W. Supramolecular modification of the periphery of dendrimers resulting in rigidity and functionality. *Angew. Chem., Int. Ed.* **2000**, *39*, 4262−4265.
(41) Broeren, M. A. C.; van Dongen, J. L. J.; Pittelkow, M.; Christensen, J. B.; van Genderen, M. H. P.; Meijer, E. W. Multivalency in the gas phase: The study of dendritic aggregates by mass spectrometry. *Angew. Chem., Int. Ed.* **2004**, *43*, 3557−3562.
(42) Banerjee, D.; Broeren, M. A. C.; van Genderen, M. H. P.; Meijer, E. W.; Rinaldi, P. L. An NMR study of the supramolecular chemistry of modified poly(propyleneimine) dendrimers. *Macromolecules* **2004**, *37*, 8313−8318.
(43) Garrett, R. H.; Grisham, C. M. *Biochemistry*; Saunders College Publishing: 1995.
(44) Stefan, M. I.; Le Novère, N. Cooperative binding. *PLoS Comput. Biol.* **2013**, *9*, e1003106.
(45) Flory, P. J. *Statistical Mechanics of Chain Molecules*; Hanser: Munich, 1989.
(46) Grosberg, A. Y.; Khokhlov, A. R. *Statistical Physics of Macromolecules*; American Institute of Physics Press: New York, 1994.
(47) Han, J.; Jaffe, R. J.; Yoon, D. Y. Conformational characteristics of polymethylene chains in melts and in various phantom chains from explicit atom molecular dynamics simulations. *Macromolecules* **1997**, *30*, 7245−7252.
(48) Huskens, J.; Mulder, A.; Auletta, T.; Nijhuis, C. A.; Ludden, M. J. W.; Reinhoudt, D. N. A model for describing the thermodynamics of multivalent host-guest interactions at interfaces. *J. Am. Chem. Soc.* **2004**, *126*, 6784−6797.
(49) Kramer, R. H.; Karpen, J. W. Spanning binding sites on allosteric proteins with polymer-linked ligand dimers. *Nature* **1998**, *395*, 710−713.
(50) Martinez-Veracoechea, F. J.; Leunissen, M. E. The entropic impact of tethering, multivalency and dynamic recruitment in systems with specific binding groups. *Soft Matter* **2013**, *9*, 3213−3219.
(51) Weber, M.; Bujotzek, A.; Haag, R. Quantifying the rebinding effect in multivalent chemical ligand-receptor systems. *J. Chem. Phys.* **2012**, *137*, 054111.
(52) Rao, J.; Lahiri, J.; Weis, R. M.; Whitesides, G. M. Design, synthesis, and characterization of a high-affinity trivalent system derived from Vancomycin and l-Lys-d-Ala-d-Ala. *J. Am. Chem. Soc.* **2000**, *122*, 2698−2710.
(53) Marrink, S. J.; Tieleman, D. P. Perspective on the Martini model. *Chem. Soc. Rev.* **2013**, *42*, 6801−6822.
(54) Lee, H.; Larson, R. G. Coarse-grained molecular dynamics studies of the concentration and size dependence of fifth- and seventh-generation PAMAM dendrimers on pore formation in DMPC bilayer. *J. Phys. Chem. B* **2008**, *112*, 7778−7784.

DOI: 10.1021/acs.macromol.8b02357
Macromolecules 2019, 52, 2778−2788